

Wear-Out Failure of a Power Electronic Converter Under Inversion and Rectification Modes

Peyghami, Saeed; Davari, Pooya; Zhou, Dao; Fotuhi-Firuzabad, Mahmud; Blaabjerg, Frede

Published in:
Proceedings of 2019 IEEE Energy Conversion Congress and Exposition (ECCE)

DOI (link to publication from Publisher):
[10.1109/ECCE.2019.8913144](https://doi.org/10.1109/ECCE.2019.8913144)

Publication date:
2019

Document Version
Early version, also known as pre-print

[Link to publication from Aalborg University](#)

Citation for published version (APA):
Peyghami, S., Davari, P., Zhou, D., Fotuhi-Firuzabad, M., & Blaabjerg, F. (2019). Wear-Out Failure of a Power Electronic Converter Under Inversion and Rectification Modes. In *Proceedings of 2019 IEEE Energy Conversion Congress and Exposition (ECCE)* (pp. 1598-1604). Article 8913144 IEEE Press.
<https://doi.org/10.1109/ECCE.2019.8913144>

General rights

Copyright and moral rights for the publications made accessible in the public portal are retained by the authors and/or other copyright owners and it is a condition of accessing publications that users recognise and abide by the legal requirements associated with these rights.

- Users may download and print one copy of any publication from the public portal for the purpose of private study or research.
- You may not further distribute the material or use it for any profit-making activity or commercial gain
- You may freely distribute the URL identifying the publication in the public portal -

Take down policy

If you believe that this document breaches copyright please contact us at vbn@aub.aau.dk providing details, and we will remove access to the work immediately and investigate your claim.

Wear-Out Failure of a Power Electronic Converter Under Inversion and Rectification Modes

Saeed Peyghami, Pooya Davari, Dao Zhou
Department of Energy Technology
Aalborg University
Aalborg, Denmark
{sap,pda,zda}@et.aau.dk

Mahmud F-Firuzabad
Electrical Engineering Department
Sharif University of Technology
Tehran, Iran
fotuhi@sharif.edu

Frede Blaabjerg
Department of Energy Technology
Aalborg University
Aalborg, Denmark
fbl@et.aau.dk

Abstract—The expected lifetime of a power electronic converter is limited by its fragile components such as semiconductor devices and capacitors. These components are prone to wear-out failures depending on the converter mission profile and component thermal characteristics. This paper explores the wear-out failure of the power converter semiconductor devices in inverting and rectifying modes of the converter using different power factors. The obtained results show the different wear-out characteristics of a converter under rectification, inversion, and also partial-inversion/rectification modes as well as when provides reactive power support. Moreover, this paper proposes B_{10} lifetime curves to estimate the converter reliability based on the operating conditions. Simulations and preliminary experiments evaluate the impact of the operating conditions for the converter reliability.

Keywords— reliability, wear-out, inverter, rectifier, lifetime, failure.

I. INTRODUCTION

Power electronics is a key enabling technology in decarbonizing and economizing the electrical energy generation and delivery systems. Power converters are used in a broad range of applications in modern power systems. However, they serve as one of the most fragile components in power systems, thus may derive significant maintenance and downtime costs [1]–[6]. Therefore, reliable design of a converter is of high importance. Recent investigations show that the semi-conductor devices and capacitors have the most contribution to the hardware failure of converters [7]. These components are prone to wear-out failures due to the thermal and power cycling induced by operating mission profiles. For instance, the number of cycles to failure in a semiconductor device is attributed to the junction temperature variation and its mean value [8]. Therefore, its expected lifetime depends on the number of cycles, junction temperature swing and mean values induced by the mission profiles. As a result, the conventional design procedure considering the rated operating condition may not guarantee to achieve a desired expected lifetime. Hence, reliability-oriented design approaches, also known as mission profile-based methods have been introduced considering the converter operating conditions [9]–[16].

Mission profile-based approaches have been applied for photovoltaic, wind and other applications with a unidirectional power flow [9]–[16]. However, in many

applications, such as battery storage systems, electrical vehicle chargers, interlinking converters in micro-grids, and multi-terminal dc grids the converters are operated in a bi-directional mode [17]. Depending on the power flow direction, the wear-out failure of components, i.e., switches and diodes, and consequently dominant component from a reliability stand-point may vary from one application to another. The switches are known as fragile components in photovoltaic and wind power inverters [9]–[14].

This paper evaluates the wear-out failure of half-bridge converter under rectification and inversion modes with different power factors. The reason for studying the half-bridge structure is the fact that this converter can be considered as the building block of various converters such as modular multilevel, single-phase and three phase two level converters, bidirectional and double-stage high frequency dc-dc converters. Therefore, understanding the wear-out behavior of this converter can be fruitful for optimal design and operation of different converter topologies with various applications. The converter structure and operation condition are explained in Section II for illustrating the impact of power factor and power flow direction on the components thermal stress. Furthermore, the mission profile-based wear-out reliability prediction approach is presented in Section III. Section IV illustrates the numerical analysis including the converter reliability and wear-out failure under different operating conditions. Moreover, experimental results are provided in Section V. Finally, the outcomes are summarized in Section VI.

II. CONVERTER STRUCTURE AND OPERATION

The half-bridge power converter structure is shown in Fig. 1 with two Insulated Gate Bipolar Transistors (IGBTs) and two anti-parallel diodes. The current sharing among different components depends on the output voltage and current polarity, and hence, the current flows through:

T_1 if $v_o(t) > 0$ and $i_o(t) > 0$,

D_1 if $v_o(t) > 0$ and $i_o(t) < 0$,

D_2 if $v_o(t) < 0$ and $i_o(t) > 0$,

T_2 if $v_o(t) < 0$ and $i_o(t) < 0$.

For instance, the current sharing between upper IGBT (T_1) and diode (D_1) is shown in Fig. 2 for inversion and rectification modes with two power factors. As it can be seen from Fig. 2(a) and (b), during inversion mode, T_1 is operating and the effective current of D_1 is very low.

Furthermore, Fig. 2(c) and (d) show the current flows through diode D_1 in the rectification mode. The impact of reactive power injection is shown in Fig. 2(b) and (d) with power factor ($\text{PF} = \cos(\varphi) = 0.85$), where in the inversion mode, the diode is operating within phase angle φ and in the rectification mode, the IGBT is conducting during phase angle φ . Therefore, the conduction losses of IGBT and diode are dependent on the power factor. In general, the conduction loss, P_c on the IGBT and diode can be found as (1) and (2) for e.g., a sinusoidal pulse width modulation [18]–[20]:

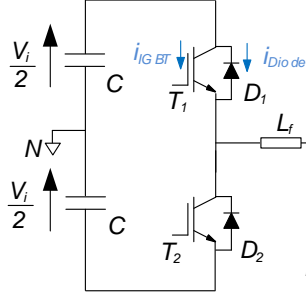


Fig. 1. Half-bridge voltage source converter.

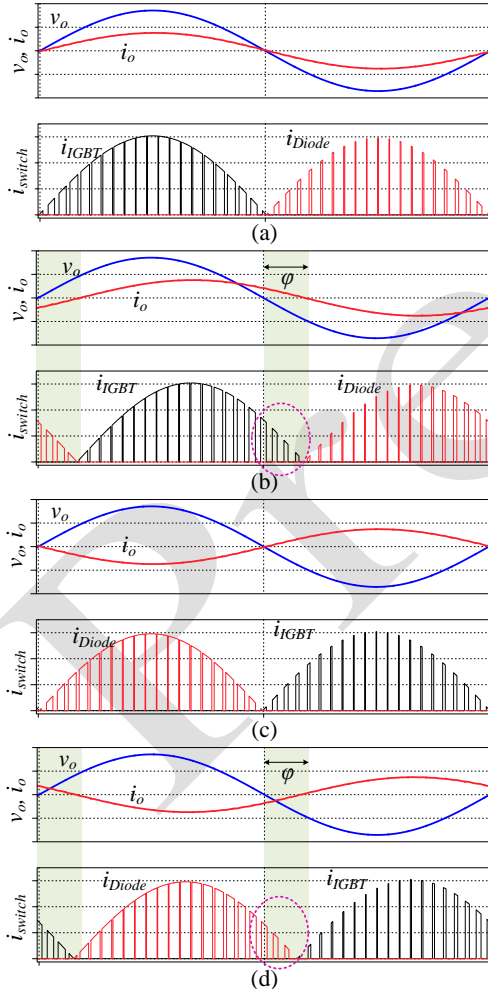


Fig. 2. Operation of voltage source converter (a) inversion mode with $\text{PF} = 1$, (b) inversion mode with $\text{PF} = 0.85$, (c) rectification operation with $\text{PF} = 1$, (d) rectification operation with $\text{PF} = 0.85$.

$$P_{C,IGBT} = \left(\frac{1}{2\pi} + \frac{m \cdot \cos(\varphi)}{8} \right) \cdot V_{CE}(T_j) \cdot \hat{i}_o + \left(\frac{1}{8} + \frac{m \cdot \cos(\varphi)}{3\pi} \right) \cdot r_{CE}(T_j) \cdot \hat{i}_o^2 \quad (1)$$

$$P_{C,Diode} = \left(\frac{1}{2\pi} - \frac{m \cdot \cos(\varphi)}{8} \right) \cdot V_F(T_j) \cdot \hat{i}_o + \left(\frac{1}{8} - \frac{m \cdot \cos(\varphi)}{3\pi} \right) \cdot r_F(T_j) \cdot \hat{i}_o^2 \quad (2)$$

where, m denotes as modulation index, V_{CE} and r_{CE} are the IGBT collector-emitter voltage and resistance, V_F and r_F are the diode forward voltage and resistance, T_j is the junction temperature, and \hat{i} is the ac side peak current.

According to (1) and (2), by increasing $0 < |\varphi| < \pi/2$, conduction loss of the IGBT will be decreased, while it will be increased for the diode. This will affect the junction temperature of the diode and IGBT as illustrated in Fig. 3 for the operating condition in Fig. 2. Fig. 3 shows the thermal behavior of the converter components under different operating conditions. During inversion mode, the IGBT junction temperature is higher than that of the diode and vice-versa for the rectification mode. For the selected IGBT, i.e., IKFW50N60DH3E, the junction temperature swing on the diode in rectifying mode is almost 38°C at 30 A peak ac current, while it is 29°C for the IGBT in inversion mode. Furthermore, the minimum junction temperatures of the IGBT and diode are also different under the applied operating conditions. These variations are attributed to the operating conditions, and the diode/IGBT thermal characteristics. The next section describes the relation between the converter thermal behavior and its reliability.

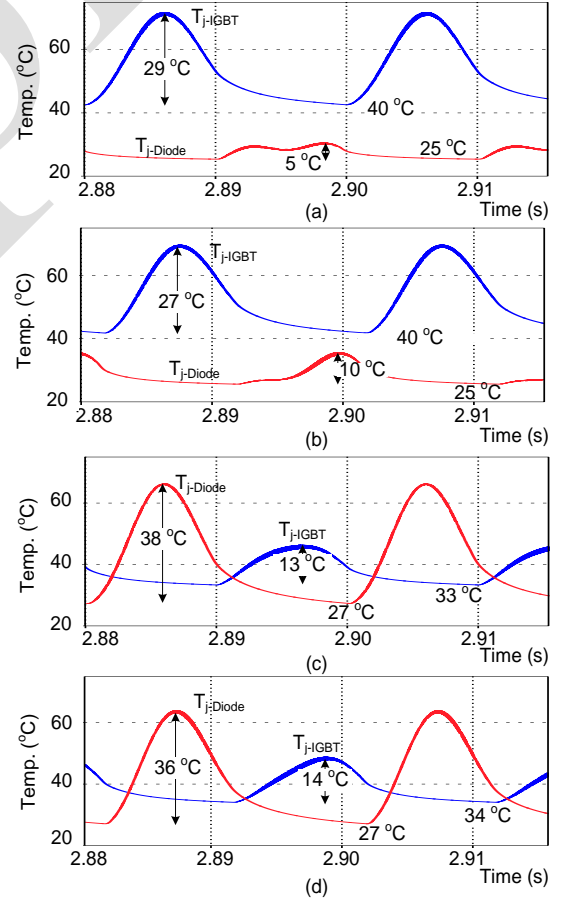


Fig. 3. IGBT and Diode junction temperatures ($^\circ\text{C}$); (a) inversion mode ($\text{PF} = 1$), (b) inversion mode ($\text{PF} = 0.85$), (c) rectification mode ($\text{PF} = 1$) and (d) rectification mode ($\text{PF} = 0.85$) – with IKFW50N60DH3E, $V_i = 400$ V, $v_o = 230$ V.

III. MISSION PROFILE BASED WEAR-OUT RELIABILITY PREDICTION

The two main factors affecting the lifetime of semiconductor devices, such as IGBT and diode, are junction temperature swing (ΔT_j) and its minimum value (T_{jm}). The number of cycles to failure (N_f) for a semiconductor device is calculated by using (3) [8].

$$N_f = A \cdot \Delta T_j^\alpha \cdot \exp\left(\frac{\beta}{T_{jm}}\right) \cdot \left(\frac{t_{on}}{1.5}\right)^{-0.3}; 0.1s \leq t_{on} \leq 60s \quad (3)$$

where, $A = 9.34 \times 10^{14}$, $\alpha = -4.416$ and $\beta = 1290$ [8], and t_{on} is the thermal heating time in each cycle [8]. The accumulated damage of the semiconductor devices (AD_s) under different power cycling is obtained using:

$$AD_s = \sum_{h=1}^H \frac{n_{cycle,h}}{N_{f,h}} \quad (4)$$

in which, $n_{cycle,h}$ is the number of cycles for h^{th} power cycle and $N_{f,h}$ is the number of cycles to failure with the operating T_{jm} and ΔT_j in the h^{th} power cycle, which is calculated using (3). H is the total number of power cycles induced by the mission profile.

Dynamic thermal variables of each power cycle on the mission profile including t_{on} , T_{jm} and ΔT_j can be translated into static variables with the same degradation on the devices [21]. These values can be employed to estimate the lifetime of a device under the applied mission profile with constant parameters in the lifetime model provided in (3). In practice, the lifetime model, the component parameters and thermal stresses have stochastic behavior, and the uncertainty on these parameters should be considered in the lifetime prediction. Therefore, Monte-Carlo simulation can be employed to estimate the failure density function of each device. In the case that more than one IGBT/Diode is used, the overall IGBTs/Diodes reliability is found by a series reliability network model assuming that if one device fails, the system fails. The overall converter reliability (R) can be found as:

$$R = R_T \times R_D \quad (5)$$

where, R_D and R_T are the reliability of diodes and IGBTs. The procedure of the reliability calculation for semiconductor devices is shown in Fig. 4 and discussed in [11]. The estimated reliability employing (3) models the device aging or degradation due to the internal failure mechanisms, such as wire bonds lift-off, under the operating condition, hence, it estimates the wear-out failures. Therefore, the converter wear-out failure rate, $h(t)$ is calculated using:

$$h(t) = \frac{-\frac{d}{dt}R(t)}{R(t)} \quad (6)$$

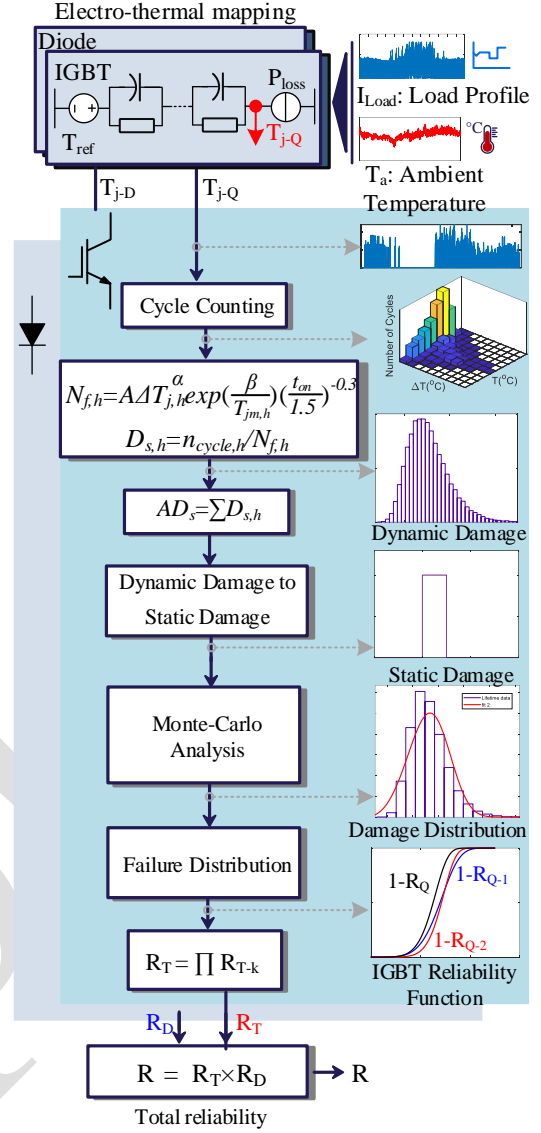


Fig. 4. Mission profile-based wear-out failure prediction procedure.

IV. COMPARATIVE ANALYSIS

The wear-out failure of converter is calculated under different loading condition as shown in Fig. 5 including full-inversion mode (Mode I), partial-inversion mode (Mode II), inversion-rectification mode (Mode III), and full-rectification mode (Mode IV). The annual converted energy with two power factor (PF) values is summarized in Table I. Notably, the annual converted energy is the absolute area under the annual power profile. For the sake of having a fair comparison, the identical load profiles are considered with the same peak power and number of cycles. Under PF = 0.85, the converter injects reactive power into the ac bus and at the rated apparent power, i.e., 3.5 kVA, the active power should be decreased to prevent overstressing the switches, and the converter is operated under constant power factor.

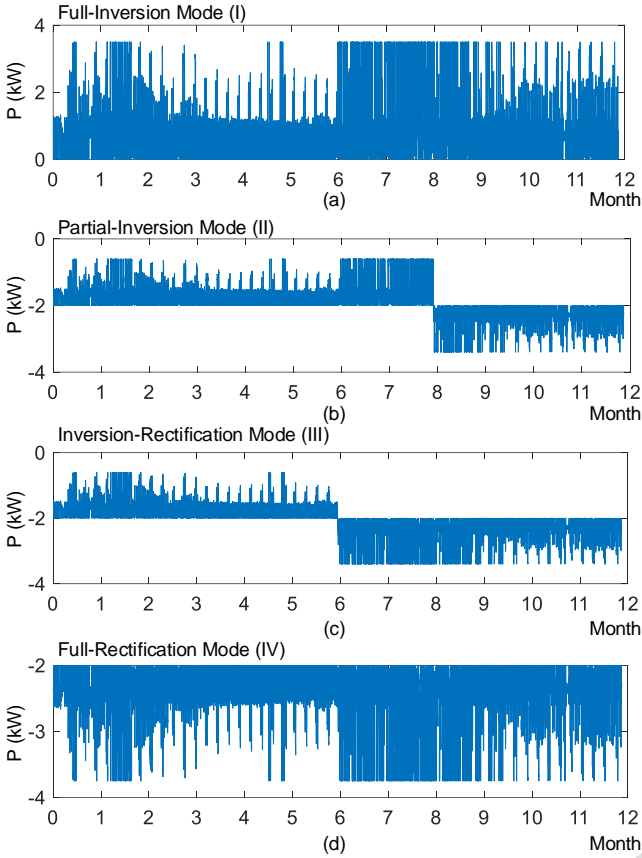


Fig. 5. Annual mission profile under (a) Full-inversion, (b) partial-inversion, (c) inversion-rectification, and (d) full-rectification modes.

Table I. Converter annual loading at different operating modes.

PF	Power flow	Mode I (MWh)	Mode II (MWh)	Mode III (MWh)	Mode IV (MWh)
0.85	Inverted	8.58	5.61	4.06	0
	Rectified	0	2.96	4.52	8.58
1	Inverted	8.75	5.72	4.10	0
	Rectified	0	3.03	4.65	8.75

Table II. Converter component parameters.

Switch	Product type	Rated current	Thermal resistance	Switching frequency
IGBT	IKFW50N60DH3E	40 A	1.15 K/W	20 kHz
Diode		40 A	2.16 K/W	
IGBT	IGW30N60TP	30 A	0.5 K/W	
Diode	IDP30E65D2	30 A	1.05 K/W	

The converter devices specifications are summarized in Table II. The effective thermal resistances of the switch and diode are also reported in Table II, while the complete thermal impedance given in the component datasheet is simulated as shown in Fig. 4.

The predicted converter reliability due to the wear-out failure is shown in Fig. 6 employing the discrete IGBT with anti-parallel diode. In the inversion mode (I), the IGBT limits the converter reliability as shown in Fig. 6(a). However, in Modes II, III, and IV, the diode has a dominant impact on the converter reliability. The total converter reliability is shown in Fig. 7(a) and the corresponding wear-out failure rate is shown in Fig. 7(b). These results show that even the rated current of components (40 A) are almost two times the peak current (20 A), the converter wear-out failure is significantly higher in the rectification mode.

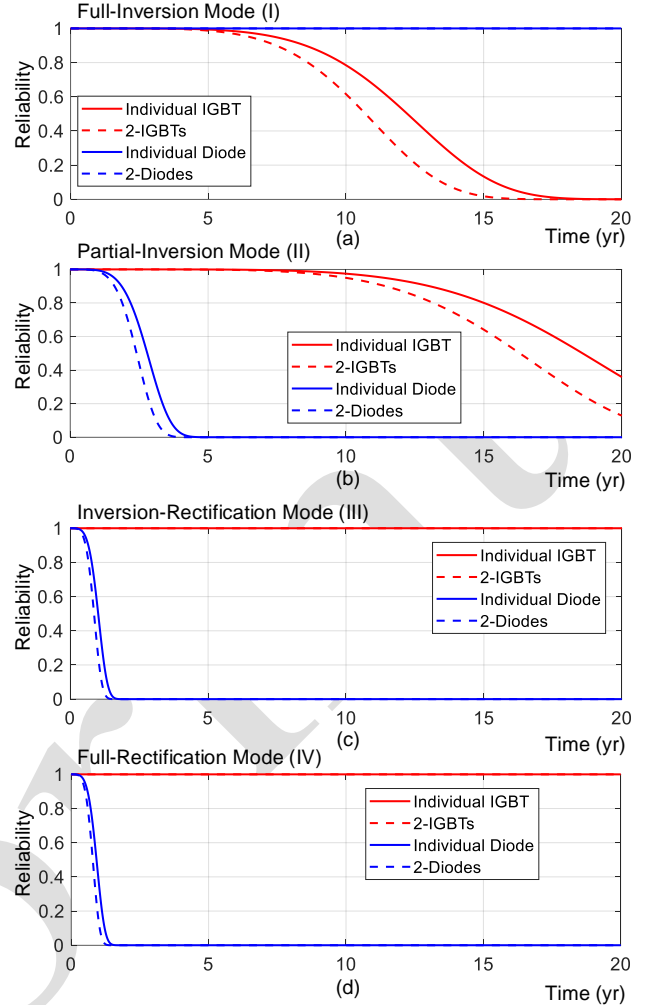


Fig. 6. Converter component reliability with IGBT-diode with PF = 1: IKFW50N60DH3E: (a) Mode I, (b) Mode II, (c) Mode III, (d) Mode IV.

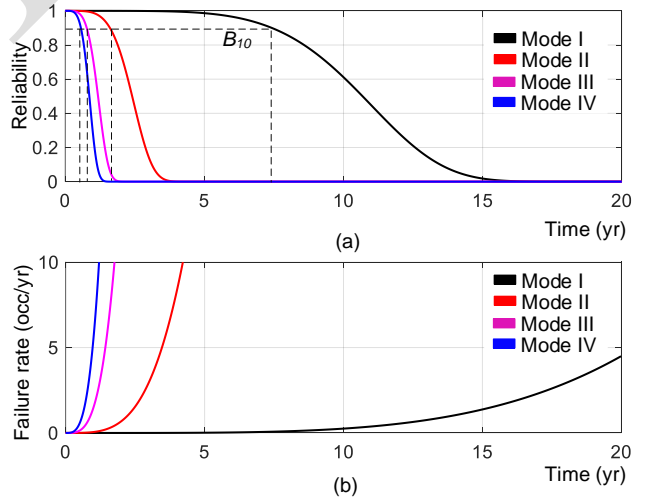


Fig. 7. Converter reliability (a) and failure rate (b) under different operating conditions employing IGBT-diode: IKFW50N60DH3E.

This is due to the higher thermal resistance of the diode – almost two times of IGBT. Therefore, even though the IGBT and diode have the same rated current of 40 A, the converter reliability under rectification mode is much lower. As a result, employing bidirectional converters, the worst-

case loading condition at both inversion and rectification modes should be taken into account during design procedure. For instance, in this case study, the diode is the failure prone component in the rectification mode. Hence, another diode with lower thermal resistor is employed as given in Table II. Moreover, a discrete IGBT is selected.

The converter reliabilities under unity power factor ($PF = 1$) and $PF = 0.85$ are shown in Fig. 8 and Fig. 9. As shown in Fig. 9 (a), in the inversion mode, the converter reliability is notably high due to the components' lower thermal resistance. Furthermore, in the rectification modes (II, III, and IV), the diode is still failure-prone component. However, the converter reliability is significantly improved. This fact is due to the diode thermal resistance, which is almost half of the previous case value as given in Table II. This study shows that even at the rated current of IGBT and diode is lower than in the previous case, the converter is more reliable. Furthermore, in the inversion-rectification mode (II), even though the inverted annual energy is almost two times the rectified energy following Table I, the diodes are still the dominant components from a wear-out failure point of view. As a result, the operating conditions such as inversion-rectification modes, mission profiles, and thermal characteristics are of high importance for converter design.

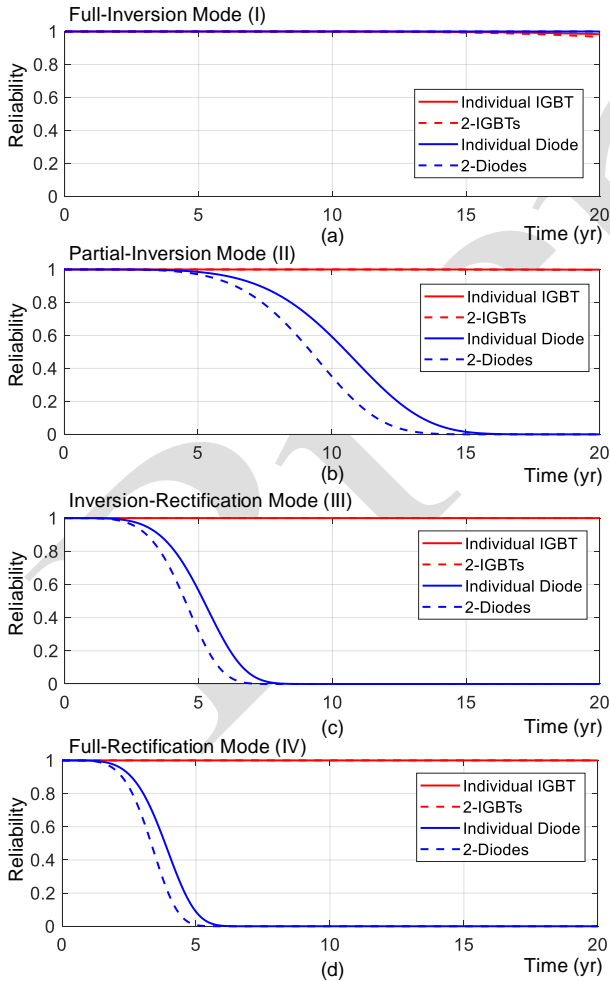


Fig. 8. Converter component reliability under $PF = 1$ with IGBT: IGW30N60TP, and diode: IDP30E65D2: (a) Mode I, (b) Mode II, (c) Mode III, (d) Mode IV.

Moreover, employing commercial inverters for bi-directional applications require detailed understanding about the thermal characteristics of the converter components, otherwise the guaranteed lifetime might not be ensured.

The impact of reactive power is further illustrated in Fig. 9, implying the converter reliability enhancement in the case of reactive power injection. As noted earlier, during reactive power support, in the rectification mode, the diode thermal stress is reduced. Fig. 10 shows the converter reliability and failure rate under unity power factor and $PF = 0.85$. This result depends on the reactive power support strategy. In this case study, it is considered that the converter has fixed power factor at 0.85 and the apparent power is limited to 3.5 kVA. However, in practice it may be operated under different reactive power supply to regulate the ac bus voltage or support the reactive loads in the grid. Therefore, in the design procedure, the reactive power mission profile must also be taken correctly into account.

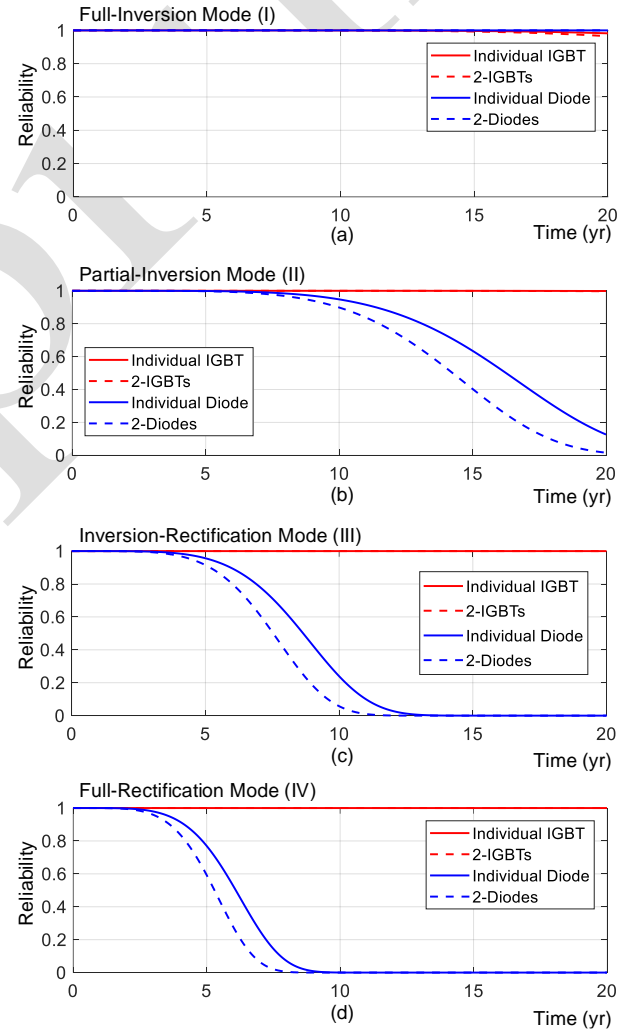


Fig. 9. Converter component reliability under $PF = 0.85$ with IGBT: IGW30N60TP, and diode: IDP30E65D2: (a) Mode I, (b) Mode II, (c) Mode III, (d) Mode IV.

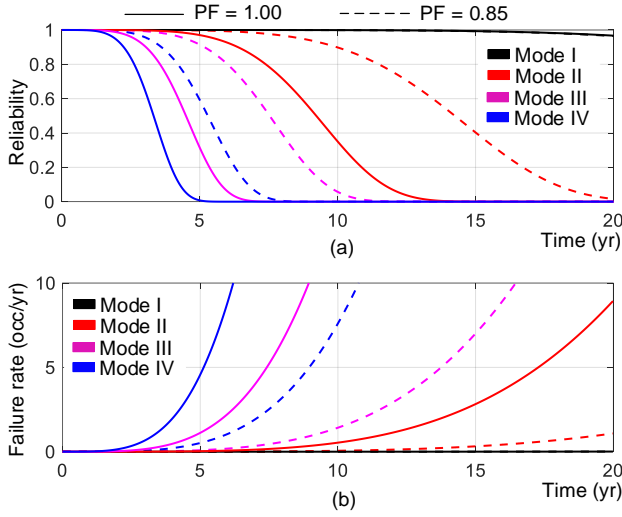


Fig. 10. Converter reliability (a) and failure rate (b) under different operating conditions employing IGBT: IGW30N60TP, and diode: IDP30E65D2.

Reliability of the converter is further illustrated by B_{10} curves for different operating points in Fig. 11. For instance, the green curve shows a set of operating points in which the converter reliability is 90% after 20 years of operation. Comparing the constant apparent power curve at 4 kVA with the constant B_{10} curves shows the impact of power flow direction and the reactive power impact on the converter reliability behavior.

As it can be seen from Fig. 11, the converter lifetime is much more limited in the rectification mode compared to the inversion mode. For instance, the B_{10} lifetime of 5 years will achieve at 3 kW rectified power, while it is achieved by 4.5 kW inverter power (see curve blue of Fig. 11). Furthermore, if the converter operated at 3.5 kVA, by increasing the phase angle ϕ from zero to π rad, the converter lifetime first moves from a 20-year curve at A (see Fig. 11) to a 40-year curve at B. Afterwards, it moves to 20-year at C, 10-year at D, 5-year at E and even shorter lifetime curves at F. This is due to the fact that the switch current will be decreased at B since the active power is reduced. Hence, the reliability is increased. Then, the diode current and consequently its thermal stress is increased. Thereby, the reliability is decreased. As a result, depending on the mission profile and operating point of the converter, its reliability can be higher/lower than the expected value.

These curves can be used to predict the converter lifetime operating in the region surrounded by each curve. In this approach, the converter loading dynamics are considered to be very slow. However, in general, the loading dynamics can also be included and may change the contours.

V. EXPERIMENTAL RESULTS

The impact of power flow direction on the thermal stress of the semiconductor devices has been experimentally demonstrated in a three-phase inverter as shown in Fig. 12. The converter has been operated under inversion and rectification modes and the junction temperature of the highlighted diode and IGBT in Fig. 12(b) is measured. Due

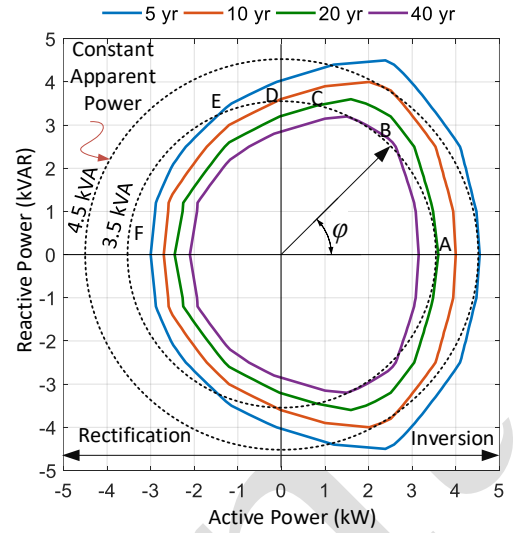


Fig. 11. B_{10} lifetime curves for different operating conditions.

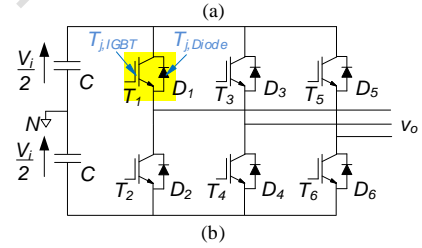
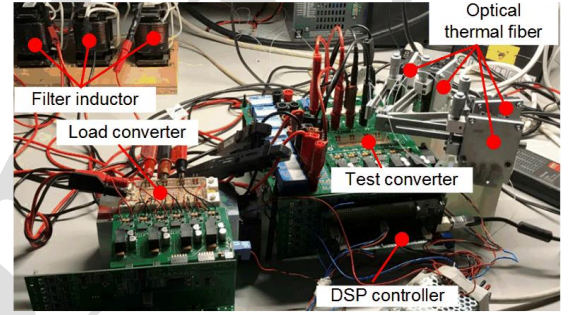


Fig. 12. Photograph of (a) test setup and (b) test converter topology.

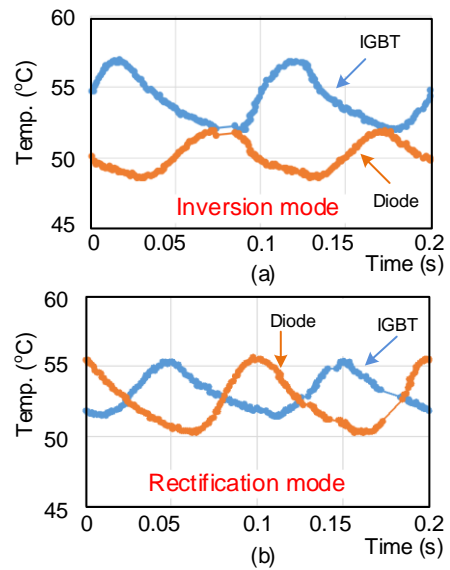


Fig. 13. Experimental results; IGBT and diode junction temperatures at: (a) inversion mode, (b) rectification mode.

to the bandwidth limit of the measurements, the fundamental frequency has been set to 10 Hz. The results are shown in Fig. 13(b) and (c) for inversion and rectification modes respectively. As it is shown in Fig. 13 (b), during inversion mode, the IGBT junction temperature is higher than the diode. Furthermore, the diode temperature swing is smaller than the IGBT. On the other hand, in the rectification mode, the diode and IGBT temperatures are almost equal while the diode temperature swing is greater than IGBT.

VI. CONCLUSION

This paper explores the wear-out failure of power electronic converters under inversion and rectification modes also when supporting reactive power. The obtained results show the wear-out failure depends on the converter operating conditions – such as power flow direction and reactive power supply – and the components thermal characteristics. Furthermore, the reactive power mission profile affects the wear-out failure of the converters. Hence, according to the specified application, the worst-case loading condition in each rectification and inversion modes should be considered during the design procedure.

The analysis shows that the current flows through the IGBTs during inversion mode, and the diodes are conducting in the rectification mode. Hence, for an inverter, the IGBTs wear-out failure should be taken into account, while in the rectification mode, the diodes are of significant importance for converter design. Moreover, during the inversion-rectification mode, IGBTs or diodes or even both of them may affect the converter failure rate depending on the mission profile and its components thermal characteristics. In the presented case studies, the diodes have the dominant impact on the total reliability in the inversion-rectification mode.

REFERENCES

- [1] K. Fischer, F. Besnard, and L. Bertling, "Reliability-Centered Maintenance for Wind Turbines Based on Statistical Analysis and Practical Experience," *IEEE Trans. Energy Convers.*, vol. 27, no. 1, pp. 184–195, Mar. 2012.
- [2] C. J. Crabtree, D. Zappalá, and S. I. Hogg, "Wind Energy: UK Experiences and Offshore Operational Challenges," *J. Power Energy*, vol. 229, no. 7, pp. 727–746, 2015.
- [3] K. Fischer, K. Pelka, A. Bartschat, B. Tegtmeier, D. Coronado, C. Broer, and J. Wenske, "Reliability of Power Converters in Wind Turbines: Exploratory Analysis of Failure and Operating Data from a Worldwide Turbine Fleet," *IEEE Trans. Power Electron.*, vol. 34, no. 7, pp. 6332–6344, 2018.
- [4] B. Hahn, M. Durstewitz, and K. Rohrig, "Reliability of Wind Turbines - Experience of 15 Years with 1500WTs," *Wind Energy*, no. January, pp. 329–332, 2005.
- [5] A. Golnas, "PV System Reliability: An Operator's Perspective," *IEEE J. Photovoltaics*, vol. 3, no. 1, pp. 416–421, 2013.
- [6] L. M. Moore and H. N. Post, "Five Years of Operating Experience at a Large, Utility-Scale Photovoltaic Generating Plant," *Prog. Photovoltaics Res. Appl.*, vol. 16, no. 3, pp. 249–259, 2008.
- [7] J. Falck, C. Felgelmacher, A. Rojko, M. Liserre, and P. Zacharias, "Reliability of Power Electronic Systems: An Industry Perspective," *IEEE Ind. Electron. Mag.*, vol. 12, no. 2, pp. 24–35, Jun. 2018.
- [8] R. Bayerer, T. Herrmann, T. Licht, J. Lutz, and M. Feller, "Model for Power Cycling Lifetime of IGBT Modules - Various Factors Influencing Lifetime," in *Proc. IEEE CIPS*, 2008, pp. 1–6.
- [9] S. Peyghami, H. Wang, P. Davari, and F. Blaabjerg, "Mission Profile Based Power Converter Reliability Analysis in a DC Power Electronic Based Power System," in *Proc. IEEE ECCE*, 2018, pp. 1–7.
- [10] F. Blaabjerg, K. Ma, D. Zhou, and Y. Yang, "Mission Profile-Oriented Reliability Design in Wind Turbine and Photovoltaic Systems," in *Reliability of Power Electronic Converter Systems*, Institution of Engineering and Technology, 2015, pp. 355–390.
- [11] S. Peyghami, P. Davari, H. Wang, and F. Blaabjerg, "The Impact of Topology and Mission Profile on the Reliability of Boost-Type Converters in PV Applications," in *Proc. IEEE COMPEL*, 2018, pp. 1–8.
- [12] S. Peyghami, P. Davari, H. Wang, and F. Blaabjerg, "System-Level Reliability Enhancement of DC/DC Stage in a Single-Phase PV Inverter," *Microelectron. Reliab.*, vol. 88–90, pp. 1030–1035, Sep. 2018.
- [13] K. Ma, M. Liserre, F. Blaabjerg, and T. Kerekes, "Thermal Loading and Lifetime Estimation for Power Device Considering Mission Profiles in Wind Power Converter," *IEEE Trans. Power Electron.*, vol. 30, no. 2, pp. 590–602, Feb. 2015.
- [14] F. Hahn, M. Andresen, G. Buticchi, and M. Liserre, "Mission Profile Based Reliability Evaluation of Building Blocks for Modular Power Converters," in *Proc. IEEE PCIM*, 2017, pp. 1017–1023.
- [15] S. Peyghami, P. Davari, and F. Blaabjerg, "System-Level Reliability-Oriented Power Sharing Strategy for DC Power Systems," *IEEE Trans. Ind. Appl.*, no. DOI:10.1109/TIA.2019.2918049, pp. 1–11, 2019.
- [16] S. Peyghami, H. Wang, P. Davari, and F. Blaabjerg, "Mission Profile Based System-Level Reliability Analysis in DC Microgrids," *IEEE Trans. Ind. Appl.*, no. DOI:10.1109/TIA.2019.2920470, pp. 1–13, 2019.
- [17] S. Peyghami, H. Mokhtari, and F. Blaabjerg, "Autonomous Operation of a Hybrid AC/DC Microgrid with Multiple Interlinking Converters," *IEEE Trans. Smart Grid*, pp. 1–1, 2017.
- [18] J. W. Kolar, E. R. T. L. Hans, and C. Zach, "Influence of the Modulation Method on the Conduction and Switching Losses of a Pwm Converter System," in *Conference Record of the 1990 IEEE Industry Applications Society Annual Meeting*, 1990, pp. 502–512.
- [19] J. W. Kolar, F. C. Zach, and F. Casanellas, "Losses in PWM Inverters Using IGBTs," *IEE Proc. - Electr. Power Appl.*, vol. 142, no. 5, pp. 285–288, 1995.
- [20] A. Wintrich, U. Nicolai, W. Tursky, and T. Reimann, "Application Manual Power Semiconductors," 2nd ed. Germany: ISLE Verlag, 2015.
- [21] J. McPherson, "Reliability Physics and Engineering," 2nd ed. Switzerland: Springer Int., 2013.